




## Fiber Bragg Grating Temperature Sensor and its Interrogation Techniques

Raja Yasir Mehmood Khan<sup>1</sup> , Rahim Ullah<sup>1</sup> , Muhammad Faisal<sup>1</sup> <sup>1</sup>National Institute of Lasers and Optronics College, Pakistan Institute of Engineering and Applied Sciences, Nilore, Islamabad, 45650, Pakistan

### Keywords

Fiber Bragg grating,  
Temperature sensor,  
Interrogation techniques,  
Optical fiber interferometry,  
Edge filters,  
TDM,  
WDM.

### Abstract

In this comprehensive review, our focus centers novel strategies and methodologies in FBG temperature sensors and their interrogation techniques investigated for sensing in different environments. FBG temperature sensors are investigated for cryogenic, ambient, high-temperature and ultrahigh-temperature environments. Interrogation techniques encompasses optical interferometry, optical edge filtering, time division multiplexing, optical spectrum analysis (OSA) and wavelength division multiplexing (WDM), each possessing distinct characteristics and working principles. The optical interferometry technique offers exceptional sensitivity and high resolution but has a relatively lower temperature sensing range. The optical edge filtering technique provides good temperature sensitivity, enhanced resolution and nominal temperature sensing range which are mainly dependent on the span and slope of the edge of the optical filter. TDM interrogation technique has the multiplexing capability and cost-effectiveness but limitations like the requirement of partial reflective matched FBGs, spatial separation of the FBGs and the potential cross-talk make it less attractive for commercial applications. OSA and WDM techniques excel in multiplexing capabilities and boast the widest temperature sensing range. However, OSA is limited for research applications only. On the other hand, WDM stands out with its cost-effective per-sensor implementation and extensive usage in commercial interrogation systems. The significance of this review lies in its ability to provide researchers, engineers, and practitioners with a coherent understanding of the evolving FBG temperature sensing landscape. By consolidating and highlighting recent breakthroughs, we aim to inspire further research initiatives and foster the development of optimized FBG temperature sensing systems.

### 1. Introduction

Temperature is a crucial factor in scientific research as it affects various physical, chemical, and biological processes. In physics, temperature is important for understanding thermal expansion, phase transitions, and the behavior of gases. In chemistry, it is critical for controlling reaction rates and the stability of compounds. In biology, temperature influences enzyme activity, metabolic rates, and the survival of organisms[1]. Additionally, temperature measurements are vital for ensuring accurate experimental results and maintaining the integrity of equipment and materials. Therefore, temperature control and measurement are essential in both industry and science to enhance efficiency, productivity, and safety. Measuring temperature is not a recent development. In fact, measuring temperature has been a fundamental component of scientific and engineering activities for many centuries. Galileo Galilei's thermoscope, which used the expansion and contraction of air to indicate temperature changes, was an early precursor to the modern thermometer. Daniel Fahrenheit's development of the mercury-in-glass thermometer in the early 18th century was a significant advancement in temperature measurement. This design, which later led to the creation of the Fahrenheit temperature scale, is still in use today. Sir Thomas Allbutt's invention of the medical thermometer in the late 19th century revolutionized the field of patient care by providing a convenient and accurate means to measure body temperature[2]. Nowadays commercially available temperature sensors are thermometers, thermo-electric thermocouples, bimetallic thermometers, and temperature-dependent resistance thermometers and these are widely deployed in many industries and lab environments [3, 4]. Conventional temperature sensors have limitations including low reliability, high

temperature fluctuations, susceptibility to electromagnetic and radiofrequency interferences, and potential fire hazards in industries involving petroleum and explosives. Over the past few decades, optical fiber sensors have gained considerable attention in research. These sensors were invented shortly after the practical optical fiber was introduced in 1970[5]. They offer advantages such as compactness, lightweight design, immunity to electromagnetic and radiofrequency interferences, as well as remote sensing and multiplexing capabilities. The multiplexing capability of optical fiber sensors allows for the connection of multiple sensors in series, using a single consolidated monitoring system. This reduces the cost per sensor and simplifies the overall setup. Optical fibers are made of insulating materials, primarily silica, making them a preferable choice in regions with high voltages compared to conventional electrical sensors. Furthermore, optical fiber sensors are passive and do not require electrical power at the location of the sensor. This passive nature makes them ideal for use in explosive and petroleum industries where the risk of fire is present. Overall, these traits make optical fiber sensors more attractive, suitable, and preferable over their conventional counterparts [5].

FBGs are a distinctive type of optical fiber sensors which were discovered unwittingly by K. Hill and co-workers in 1978 [5]. They found a weak inscription of gratings in core of a photosensitive fiber by launching a beam of 488 nm argon laser. In another experiment they found strong gratings in core of a photosensitive fiber by launching high power blue light through it. FBGs are periodically disseminated reflectors in a short segment of core of an optical fiber (as shown in figure 1(a)). FBGs are broadly created by three techniques: (i) interferometry technique, (ii) phase mask technique and (iii) point by point laser inscription scheme [6, 7]. In interferometry technique a germanium doped (photo-sensitive) optical fiber is exposed to

\*Corresponding Author: [mfaisal13@yahoo.com](mailto:mfaisal13@yahoo.com)

Received 18 May 2023; Revised 01 Sep 2023; Accepted 01 Sep 2023

2687-5195 /© 2022 The Authors, Published by ACA Publishing; a trademark of ACADEMY Ltd. All rights reserved.

<https://doi.org/10.36937/ben.2023.4840>

interference fringes produced by diffraction gratings. Hologram of diffraction gratings is permanently printed on the core of the optical fiber. Holographic inscription technique is not suitable because interferometry is very perceptible to even a minute vibration and also batch-to-batch production of FBGs is not possible by this technique. In phase mask technique the photosensitive fiber is exposed to diffraction pattern produced from phase mask by a pulsed UV laser beam. In phase mask technique strong gratings can also be produced on single mode fiber (SMF-28) by using femto-second laser and phase mask. Phase mask technique is being used for commercial high-volume production of FBGs from decades. In point by point inscription, FBGs are written by using femto-second laser without aid of phase mask [8].

On exposure to light from a broad band source (BBS), an FBG reflects a particular wavelength termed as Bragg wavelength or central wavelength ( $\lambda_B$ ) and remaining spectrum is transmitted. Working of an FBG is similar to X-rays diffraction from a intermittent crystal structure (as shown in figure 1(b)). By Bragg's law, diffraction of X-rays occurs when wavelength ( $\lambda$ ) of the rays is analogous to interatomic spacing ( $d$ ) of the crystal. Mathematically Bragg's Law is:

$$2d\sin\theta = n\lambda \tag{1}$$

Where ' $\theta$ ' is angle of incident of X-rays and ' $n$ ' is an integer which depicts order of diffraction. Equation (1) is also known as Bragg's condition. On satisfaction of Bragg's condition, diffracted beams from the crystal interfere constructively and an intense peak appears in the detector known as Bragg peak.

Similarly to X-rays diffraction from a crystal lattice, when an FBG is exposed to a broad band spectrum of light then each grating plane weakly reflects light and these reflected beams superpose with each other. Superposition of the beams result in constructive or destructive interferences depending on whether the reflected beams meet Bragg's condition or not. Depending on spacing between grating planes called grating period ( $\Lambda$ ) and effective refractive index ( $n_{eff}$ ) of core of the fiber light of a particular wavelength (Bragg wavelength( $\lambda_B$ )) undergoes constructive interference.

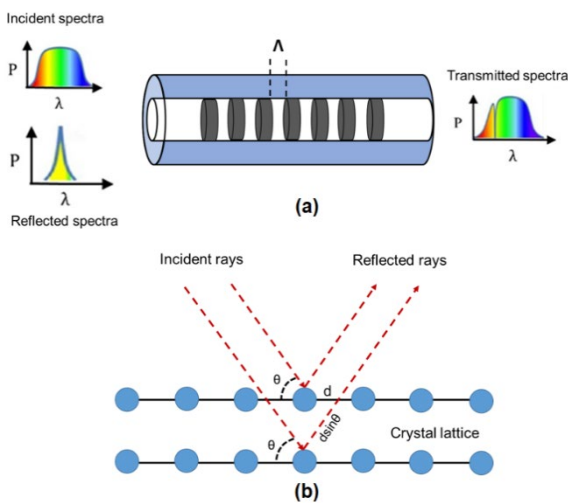


Figure 1. (a) Schematic representation of the working principle of an FBG. On exposure to a Broadband Spectrum, Bragg wavelength is reflected and remaining spectrum is transmitted. (b) Bragg's diffraction of X-rays from a crystal lattice.

This constructive interference results in a peak in reflection spectra or dip in transmission spectra of the FBG. In case of an FBG,  $\theta=90^\circ$ ,  $d=\Lambda$  and  $n=1$ . Beside  $\theta$ ,  $\Lambda$  and  $n$ , effective refractive index ( $n_{eff}$ ) of core of the fiber also alters the reflected wavelength. Effective refractive index is contingent to core and cladding refractive indexes and calculated by their average. Considering all these factors Bragg's equation for FBGs becomes [5, 9]:

$$\lambda_B = 2n_{eff} \Lambda \tag{2}$$

Bragg wavelength is directly contingent to grating period and effective refractive index of core of the fiber while grating period and

effective refractive index are dependent on physical parameters like strain and temperature etc.

On heating, changes in grating period and effective refractive index of an FBG occur, which result in variation of its Bragg wavelength ( $\Delta\lambda_B$ ). Variation in  $\Delta\lambda_B$  with change in temperature ( $\Delta T$ ) can be expressed as:

$$\frac{\Delta\lambda_B}{\Delta T} = 2n_{eff} \frac{\partial\Lambda}{\partial T} + 2\Lambda \frac{\partial n_{eff}}{\partial T} \tag{3}$$

From equation (2) using values of  $2n_{eff}$  and  $2\Lambda$  in equation (3), we have:

$$\frac{\Delta\lambda_B}{\Delta T} = \lambda_B \left( \frac{1}{\Lambda} \frac{\partial\Lambda}{\partial T} + \frac{1}{n_{eff}} \frac{\partial n_{eff}}{\partial T} \right) \tag{4}$$

Here,  $\alpha = \frac{1}{\Lambda} \frac{\partial\Lambda}{\partial T}$  and  $\xi = \frac{1}{n_{eff}} \frac{\partial n_{eff}}{\partial T}$  are thermal expansion and thermo-optic coefficients of the fiber. Equation (4) is simplified as:

$$\Delta\lambda_B = \lambda_B (\alpha + \xi) \Delta T \tag{5}$$

Similarly with strain  $\epsilon$ , variation in Bragg wavelength of an FBG is:

$$\frac{\Delta\lambda_B}{\Delta\epsilon} = 2n_{eff} \frac{\partial\Lambda}{\partial\epsilon} \Delta\epsilon + 2\Lambda \frac{\partial n_{eff}}{\partial\epsilon} \Delta\epsilon \tag{6}$$

From equation (2), using values of  $2n_{eff}$  and  $2\Lambda$  in equation (6), we have:

$$\frac{\Delta\lambda_B}{\Delta\epsilon} = \lambda_B \left( \frac{1}{\Lambda} \frac{\partial\Lambda}{\partial\epsilon} + \frac{1}{n_{eff}} \frac{\partial n_{eff}}{\partial\epsilon} \right) \tag{7}$$

In above equation (7), the term  $\frac{1}{\Lambda} \frac{\partial\Lambda}{\partial\epsilon}$  is the displacement of gratings period with strain in optical fiber in which the FBG is inscribed. As displacement of grating period is same as the strain in the fiber, therefore, this term is equal to 1. While, the term  $\frac{1}{n_{eff}} \frac{\partial n_{eff}}{\partial\epsilon}$  represents variation of effective refractive index with strain which represents opto-elastic coefficient ( $p_e$ ) of the FBG. In solids, opto-elastic coefficient is negative because when a transparent solid such as optical fiber is expanded then its refractive index decreases due to decrease in its density [5]. Using these results in equation (7), we have:

$$\Delta\lambda_B = \lambda_B (1 - p_e) \Delta\epsilon \tag{8}$$

Combining equation (5) and equation (8), variation in Bragg wavelength of an FBG due to temperature and strain is:

$$\Delta\lambda_B = \lambda_B (\alpha + \xi) \Delta T + \lambda_B (1 - p_e) \Delta\epsilon \tag{9}$$

Strain and temperature are independent of each other. By secluding temperature, FBG can be used as a strain sensor and vice versa. By calibrating change in Bragg wavelength with strain and temperature, an FBG is deployed as a strain or a temperature sensor.

This review delves into the contemporary advancements in FBG temperature sensors and their associated interrogation techniques. The primary motivation behind this review is to elucidate the novel strategies and methodologies that have surfaced in recent year. The article consists of two main sections. The first section primarily focuses on the practical uses of FBG temperature sensors in various temperature environments, including cryogenic, high temperature and ultra-high temperature environments. Additionally, in the first part, an overview of the different processing techniques applied to FBGs to enhance their functionality for temperature sensing in these extreme environments is provided. On the other hand, the second section of the review is dedicated to discussing different interrogation techniques used to extract temperature information from FBG sensors.

## 2. FBG Temperature Sensors for Different Sensing Environments

### 2.1. Cryogenic Environments

Environments with temperature in range from 128 K (-150 °C) to absolute zero (0 K or -273 °C) falls under the category of cryogenic environments. The investigation of cryogenic temperatures in superconductors and superconductor magnets is crucial for their proper construction, effective design, and adequate protection. In the past few decades, FBG sensors have been extensively researched for their applications in temperature sensing in cryogenic environments,

owing to their numerous advantages over conventional electrical sensors. These advantages include their miniature size, immunity to electromagnetic and radiofrequency interferences (EMI), and passive nature. The compact size of FBG sensors allows for easy integration into various systems, while their immunity to EMI ensures accurate and reliable temperature measurements without interference. Furthermore, FBG sensors being passive in nature do not require an external power source, enhancing their practicality in cryogenic settings. This ongoing research highlights the potential of FBG sensors as a valuable tool for temperature sensing in cryogenic environments, with the aim of advancing scientific and technological advancements in this field. Due to low temperature sensitivity at cryogenic temperatures, FBGs can't be used in bare form. Also the materials of the fiber (glass) become significantly brittle and prone to fracture due to the reduction in its molecular mobility and flexibility at temperature below its brittle transition point. Lower temperature sensitivity of FBGs at cryogenic temperatures is due to fact that with decrease in temperature thermal expansion coefficient of constituent material of fibers (silica) decreases and results in lowering temperature sensitivity of FBGs in cryogenic temperature zones [10]. To use FBG temperature sensors in cryogenic environments polymer and metal coatings are applied. In polymer coating materials like Teflon, poly methyl methane, acrylate, epoxy resin etc [11] are used. S. Parne et al.[12] coated FBG with Teflon and enabled it to sense cryogenic temperature up to 77 K. In their experiment they reported temperature sensitivity of 12.85 pm/°C and 99.2 % linearity of the sensor with temperature variation from 298 K to 77 K. D. Sengupta et al.[13] coated an FBG with Polymethyle methacrylate at room temperature and reported cryogenic temperature sensing up to 77 K with temperature sensitivity of 39 pm/K. U. Sampath et al.[11] coated FBG with acrylate and epoxy resin and reported temperature sensing up to 77 K. Sensitivities of their developed sensors were found to be 20 pm/°C and 49 pm/°C with acrylate and epoxy resin coatings, respectively in temperature range from 298 K to 77 K. Polymer coating result in enhance in temperature sensitivity than bare FBGs but does not remain sensitive enough below 77 K [14]. In metal coating tin, indium, lead, aluminum, copper, mercury etc are used [15].

In a study by C. Y. Hsu et al.[16] FBGs were coated with titanium nitride to assess their temperature sensing capabilities in cryogenic environments. The researchers found that the sensor exhibited a temperature sensitivity of 10.713 pm/°C and achieved 99.5% linearity within the temperature range of 298 K to 78 K. In another study by A.C. Soman et al.[17] Proposed the use of copper coating on FBGs and investigated the performance of copper-coated FBGs with varying copper thicknesses in the temperature range of 30 K to 100 K. The researchers achieved a maximum temperature sensitivity of 162.7 pm/K for the copper-coated FBGs mentioned above. In a study conducted by R.R. Kumar et al.[10], FBGs were coated with various metals including gold, aluminum, indium, lead, and copper, and their temperature sensing capabilities were investigated at temperatures below 15 K. The researchers found that the indium-coated FBGs exhibited higher sensitivity in temperature sensing within this temperature range. Through optimization, the indium-coated FBGs proved to be particularly effective for temperature sensing applications up to 15 K.

Metallic coating results in stability and better temperature sensitivity of FBG sensors in cryogenic environments. By using indium coating, lower temperature sensing limit is achieved up to 15 K with sensitivity of 15 pm/K [10].

## 2.2. High Temperature Environments

A high temperature environment is typically defined as an environment with temperatures ranging from above ambient temperature up to 800°C. In temperature sensing applications, standard type-I FBGs are commonly used. These type-I FBGs are created by isotropic modulation of the refractive index of the fiber through exposure to UV, nanosecond, or femtosecond laser beams. They are considered positive index gratings. However, it's worth noting that type-I FBGs due to their partial modulation of refractive index have limitations when it comes to withstanding high temperatures in their bare form. As a result, their applications in high temperature environments are restricted. However, type-I FBGs are usually further processed for high temperature applications. This processing involves: (i) Encapsulation, (ii) Coating and (iii) Regeneration.

In encapsulation technique, type-I FBGs are encapsulated in capillaries of metals like stainless steel, copper, Inconel and ceramics like silicon carbide, aluminum carbide, double thimble type encapsulation etc which enables FBGs to use in environments with temperature from 500 to 700 °C. V.R Mamidi et al.[18] conducted research on temperature sensing using type-I FBGs encapsulated in different materials. They enclosed a type-I FBG in an aluminum nitride capillary and achieved high-temperature sensing from 20 °C to 500 °C. In another study[19], they encapsulated a type-I FBG in a copper capillary and reported temperature sensing from 20 °C to 550 °C. More recently, our research group introduced a double-thimble type encapsulation for type-I FBGs, enabling temperature sensing from 30 °C to 700 °C[20]. In encapsulation technique ideal properties of FBGs like grating and mechanical strength, high reflectivity, easy appodization etc remain preserved. Also in encapsulation one end of the encapsulated FBG is kept free which immunizes it from external stresses and stresses in bodies of the encapsulated structures.

In coating techniques, type-I FBGs are commonly subjected to coatings using either polymers or metals. Polymeric coatings have been particularly effective for high-temperature sensing, with acrylate and polyimide coatings being widely studied. Pioneering work by P. Lu et al.[21] involved the application of an acrylate coating on an FBG, enabling temperature sensing capabilities of up to 100 °C with an impressive temperature sensitivity of 10.2 pm/°C. Another notable study by L. Huang et al.[22] explored the use of a polyimide coating, extending the temperature sensing range to a remarkable 350 °C. In metal coating technique metals like gold, aluminum, copper etc have been used which enhanced temperature sensing range of the FBGs up to 800 °C [23]. K.N Koo et al.[24] applied nanolayer coating of copper to FBGs. In their experiment they produced three FBGs in single mode, step index and graded index multimode fibers. They reported temperature sensing from 30 °C to 80 °C and found an increase in temperature sensitivity with increase in thickness of copper nanolayer. N F Mansor et al.[25] applied zinc oxide and silicon carbide coatings to FBGs by magnetron sputtering technique for plasma temperature measurement. They reported temperature sensing from 50 °C to 300 °C with temperature sensitivities of 12.6 pm/°C and 12.37 pm/°C for zinc oxide and silicon carbide respectively. The study conducted by X. Wang et al.[26] focuses on enhancing the temperature sensing range of FBGs up to 800 °C without compromising the thermal stability of the coated FBGs. The researchers achieved this by utilizing a metallic coating technique, specifically electroplating, with four different metals: zinc, copper, nickel, and silver. By applying these metal coatings to the FBGs, the temperature sensing range was significantly extended. This is particularly useful in applications where higher temperature measurements are required. The researchers carefully selected the four metals mentioned, as they have specific characteristics that make them suitable for this purpose. Overall, the study demonstrates the effectiveness of metallic coating, specifically electroplating, in enhancing the temperature sensing capabilities of FBGs. This advancement opens up new possibilities for using FBGs in high-temperature environments without compromising their thermal stability.

In the regeneration technique, type-I FBGs undergo annealing at high temperatures, such as 700 °C, for a specific duration. This annealing process leads to the complete decay of the FBG due to thermal effects. However, as a result of this decay, a new thermally stable FBG is formed, which can be utilized for high-temperature sensing applications, reaching temperatures as high as 600 °C.

In addition to the processing of type-I FBGs, other types such as type-IIA (type-In) FBGs have also been investigated for high-temperature applications. Type-IIA FBGs are characterized by negative index gratings and are formed in hydrogen-free silica fibers through a regeneration process. Notably, N. Groothoff et al.[27] conducted a study in which they synthesized a type-IIA FBG using boron and germanium codoped silicate fiber. They reported the capability of temperature sensing up to 800 °C, along with moderate thermal stability, lasting approximately 2.9 hours.

## 2.3. Ultra-high Temperature Environments

An environment with temperature above 800 °C is classified as a ultra-high temperature environment. Due to thermal decay phenomenon in FBGs, to use them in high and ultra-high temperature applications special treatments like regeneration etc. are required. Special FBGs like type-II, type-III and sapphire FBGs have been developed for ultra-high temperature environments. Type-II and type-III FBGs are written by using femto-second lasers (therefore also

called femto-second FBGs) by using either phase mask or point-by-point inscription. Sapphire FBGs (Fiber Bragg Gratings) are created by using femto-second lasers to write the grating structure on sapphire optical fibers. These fibers are made of single-crystalline aluminum oxide, which has a higher melting point than silica fibers commonly used in traditional FBGs. This allows sapphire FBGs to operate at higher temperatures and in more extreme environments than standard FBGs.

J. Kumar et al.[28] reported regeneration of seed type-I FBG. They reported temperature sensing capability of the devided sensor up to 900 °C in a nuclear fuel cycle facility with temperature sensitivity varying from 10.2 pm/°C to 13.72 pm/°C and life-time of ~4 years. C Zhu et al.[29] inscribed a femtosecond FBG by point-by-point inscription technique and reported survivability of the FBG up to 1000 °C. N. Chanet et al.[30] developed temperature sensing probe based on femtosecond inscribed FBG and intergrated in cooled ITER-like plasma facing component. They reported temperature sensing of the probe up to 1200 °C. M. Wang et al.[31] used femtosecond laser inscription technique to inscribe an FBG in silica core optical fiber and achieved temperature sensing up to 1000 °C. A. Martinez et al.[32] inscribed an FBG by using infrared femtosecond laser by point-by-point inscription method and reported temperature sensing up to 1200 °C. T. Habisreuther et al. [33] inscribed a sapphire FBG in a multimode single crystalline sapphire fiber by using femtosecond laser. They reported temperature sensing up to 1900 °C with temperature sensitivities varying from 23 pm/K to 35 pm/K with temperature variation from room temperature to 1500 °C, respectively.

### 3. Interrogation Techniques for FBG Temperature Sensors

On exposure to BBS light source, an FBG reflects Bragg wavelength. The Bragg wavelength is of importance because it carries information about the local measurands. Techniques which are used to measure shift in Bragg wavelength with measurands are termed as interrogation techniques. In these techniques the shift in Bragg wavelength, variation in reflected power, time taken by the Bragg wavelength to return to the monitoring system or phase shift with a measurand etc. are used to get quantitative information of the measurands. Interrogation techniques for FBG sensors are grouped in two categories: (1) Spectral demodulation and (2) Intensity demodulation. In spectral demodulation the reflected spectra of FBG sensors is detected and each peak represents a separate FBG sensor. In intensity demodulation, after filtering the transmitted light by an optical filter, the reflected spectra are detected in terms of intensity or power. Variation in intensity or power or voltage is used to get information about measurands. Spectral demodulation includes time division multiplexing (TDM), optical spectrum analyzer (OSA) interrogation, and wavelength division multiplexing (WDM) interrogation techniques. While intensity demodulation includes optical interferometry, optical edge filters and tunable filters techniques. Interrogation techniques used in FBG based temperature sensors are following:

#### 3.1. Interferometric Interrogation Technique

Interferometry based interrogation technique for FBG sensors is based on fiber Mech-Zehnder interferometer (F-MZI). Schematically an F-MZI as an interrogator for FBG sensors is shown in figure 2(a).

An F-MZI works on the principle of conversion of Bragg wavelength shift into phase shift which is further converted into intensity variations by aid of photodiodes. Reflected light (Bragg wavelength) from an FBG is divided into two beams from coupler-1 which propagate in two arms of the couple-1. These two beams interfere at output of couple-2. Outputs ( $O_1$  and  $O_2$ ) at output arms of the couplers-2 are [34]:

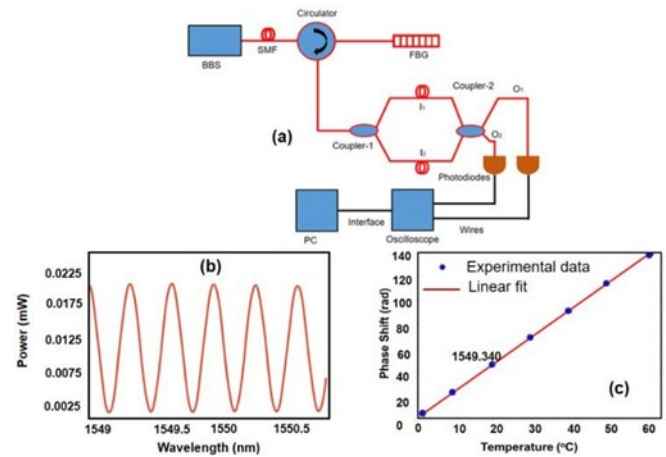


Figure 2.(a) Schematic of fiber Mach-Zehnder Interferometer Based Interrogation Technique for FBG sensors [34]. (b) Power spectrum of F-MZI recorded by OSA[34].(c)Phase shift for a F-MZI as a function of temperature[35].

$$O_1 = I_1 + I_2 + 2\sqrt{I_1 \cdot I_2} \cos \Delta\phi \quad (10)$$

$$O_2 = I_1 + I_2 + 2\sqrt{I_1 \cdot I_2} \cos(\Delta\phi - \pi) \quad (11)$$

Here,  $I_1$  and  $I_2$  are intensities of reflected light in arm-1 and arm-2 of the first coupler respectively, and  $\Delta\phi$  is phase difference. For an FBG,  $\Delta\phi$  is given as [34, 35]:

$$\Delta\phi = \frac{2\pi n_{eff} \Delta L}{\lambda_B^2} \Delta \lambda_B \quad (12)$$

here,  $n_{eff} \cdot \Delta L$  is the optical path difference between the two arms. From equation (12), shift in Bragg wavelength of an FBG by measurand (like temperature, pressure, strain etc) results in phase shift of the interferometer and causes intensity variation leading to variation in output of the photodiodes (voltage). The calibration process involves adjusting the intensity or voltage in relation to the measurand and sensor. To measure the measurand, an interferometry interrogation technique can be utilized. This technique relies on changes in intensity, making it crucial to address intensity fluctuations. These fluctuations can be caused by the phase shift of the interferometer, as well as variations in the intensity of the light source. Therefore, it is necessary to compensate for the fluctuations in the light source's intensity. To compensate intensity fluctuations, rational output method is used. Rational output is given as:

$$Rational\ Output = \frac{O_1 - O_2}{O_1 + O_2} \quad (13)$$

For  $I_1=I_2$ , rational output is:

$$Rational\ Output = \cos \Delta\phi \quad (14)$$

From equation (14), rational output is independent of intensity and only dependent to phase shift and any fluctuation in source intensity doesn't affect the output.

B. Das et al.[34] developed an interrogation technique for FBG sensors utilizing F-MZI (Fabry-Perot Michelson Interferometer) and compared it with a commercially available spectrometer interrogator through experimental analysis. Based on their study, they concluded that the F-MZI interrogator can achieve precise picometer wavelength detection, comparable to commercial spectrometers. In a further study, M. Perry et al.[35] extended the fiber interferometry interrogation technique for FBG sensors and assessed its multiplexing capability. They conducted experiments using this technique to measure strain and temperature. For temperature measurement, they employed the technique with an FBG temperature sensor within a temperature range of 0°C to 60°C. The results showed a linear variation in phase shift with increasing temperature, with a sensitivity of 2.28 rad/°C.

Interrogation techniques based on light interferometers offer several advantages, including the ability to achieve high and adjustable sensitivity, high resolution, and wide bandwidth. However, these techniques also come with some drawbacks. One of these is a limited

sensing range, which means they may not be suitable for measuring certain parameters beyond a certain range. Additionally, light interferometry techniques are highly susceptible to environmental fluctuations, commonly referred to as signal fading effects. External factors such as vibrations, air currents, and temperature variations can strongly impact the accuracy and reliability of the measurements obtained using these techniques.

### 3.2. Optical Filters-based Interrogation Techniques

Optical filters interrogation techniques utilize a slope filter to convert wavelength shifts into intensity variations. These techniques rely on the known pass and reject intensities of optical filters, which vary with the wavelength. By measuring the intensity variations, quantitative measurements of various measurands such as temperature, strain and pressure can be determined. Specifically, for FBG temperature sensors, the applied optical filters include: (i) Twin FBG[36] (ii) Long period fiber grating (LPFG) [19, 37] and (iii) Chirped fiber Bragg grating (CFBG)[38].

#### 3.2.1. Twin FBGs Interrogation Technique

The twin FBGs interrogation technique involves the use of two FBGs with similar Bragg wavelengths. One of the FBGs functions as a filter, while the other acts as a sensor. The output power is dependent on the decoupling of the Bragg spectra of the filter and the sensing FBG. Schematic of twin FBGs interrogation technique is shown in figure 3.

In the twins FBGs interrogation technique, a broadband spectrum of light is projected by the broadband source (BBS) into a single-mode fiber (SMF) towards a sensing FBG (SFBG). The spectrum then reaches the filter FBG, which reflects a specific wavelength based on its Bragg wavelength. Since both the filter and sensing FBGs are twins with the same Bragg wavelength, the power reaching the SFBG is minimized under ambient conditions. As a result, the reflected power from the SFBG is also minimized, leading to a minimum voltage output from the photodiode. However, when there is a change in the measurand (such as temperature or strain), the Bragg wavelength of the SFBG shifts, causing the Bragg spectra of the SFBG to decouple from the Bragg spectra of the filter FBG. The reflected power and output voltage are then dependent on the degree of decoupling of the spectra (as shown in figure 4).

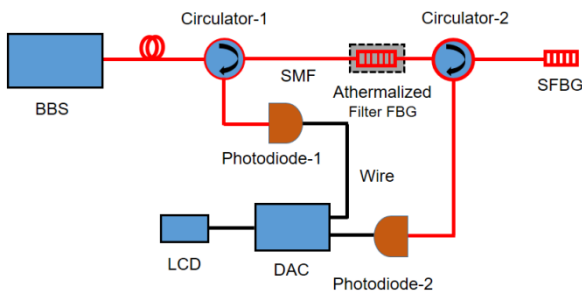


Figure 3. Schematic of Twin FBGs based Interrogation Technique for FBG Sensors[38]

J. Cui et al.[36] have developed an efficient method of interrogation using twin or matched FBGs. This method offers a fast response and high resolution. The proposed interrogator was analyzed both theoretically and experimentally, achieving a resolution of 0.3 pm, a measurable range of 60 pm, and a response speed of 500 KHz. In a recent study, our research group developed a temperature sensor package utilizing the twin FBGs-based interrogator. This package is capable of operating in a temperature range of 30 °C to 50 °C, providing a temperature resolution of approximately 0.02 °C and a maximum temperature sensitivity of 26 mV/°C[38].

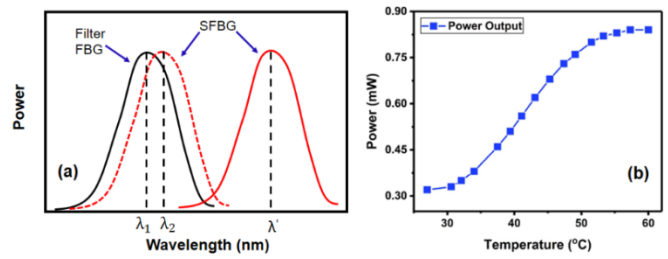


Figure 4. (a) Schematic representation of Bragg Spectra of sensing FBG (SFBG) filtered from the filter FBG in Twin FBGs interrogation Technique. (b) Output of twin FBGs interrogation technique[36].

Mathematically, reflection spectra of an FBG is given as [36]:

$$I(\lambda) = \exp \left[ -4 \ln 2 \left( \frac{\lambda - \lambda_B}{\Delta \lambda} \right)^2 \right] \tag{15}$$

where, 'λ<sub>B</sub>' is Bragg wavelength and 'Δλ' is FWHM of the FBG. Integrating equation (15), reflected power of the FBG is [36]:

$$P = \Delta \lambda \sqrt{\frac{\pi}{4 \ln 2}} \tag{16}$$

In case of twin FBGs interrogation technique, decoupling power of filter and sensing FBG is[36]:

$$P = \frac{\exp \left[ -4 \ln 2 \frac{(\lambda_1 - \lambda_2)^2}{\Delta \lambda_1^2 + \Delta \lambda_2^2} \right]}{\sqrt{\frac{4 \ln 2}{\pi} \left( \frac{1}{\Delta \lambda_1^2 + \Delta \lambda_2^2} \right)}} \tag{17}$$

where, 'λ<sub>1</sub>' and 'λ<sub>2</sub>' correspond to central wavelengths and 'Δλ<sub>1</sub>' and 'Δλ<sub>2</sub>' are the FWHM of the sensing and reference FBGs, respectively. In equation (17) term λ<sub>1</sub>-λ<sub>2</sub> represents decoupling of reflection spectra of SFBG from the filter FBG. More the decoupling, greater will be the reflected power.

Initially, the output power in the twin FBGs interrogation technique is minimum. However, as the temperature increases, the output power also increases, as depicted in figure 4(b). Once the spectra of both FBGs completely decouple from each other, the output power becomes constant. In this technique, the working range is limited to the linear region, which is determined by the full width at half maximum (FWHM) of the FBGs. Typically, FBGs have a low FWHM (≈0.3), and the linear region has a wavelength span (Δλ<sub>B</sub>) of 60 pm [37]. The temperature sensing range for FBGs can be calculated using a specific formula[5]:

$$\frac{\Delta \lambda_B}{\Delta T} = 14.18 \text{ (pm/}^\circ\text{C)} \tag{18}$$

According to equation (18), the temperature sensing range (ΔT) calculated for the interrogation technique utilizing twin FBGs is 4.23 °C. However, it has been reported that by lowering the sensitivity of the FBGs, a temperature sensing range of up to approximately 20 °C can be achieved in the twin FBGs interrogation technique [38].

Twin FBGs interrogation technique is also dependent on intensity fluctuations of source. To overcome source fluctuations rational output method is used. Rational output is given as [19]:

$$\text{Rational output} = \frac{PD_2 - PD_1}{PD_2 + PD_1} \tag{19}$$

where, PD<sub>1</sub> and PD<sub>2</sub> are outputs of photodiode-1 and photodiode-2, respectively. Filter FBG is usually athermalized by encapsulating it with an insulator like teflon etc. to protect it from variation of external environmental temperature.

#### 3.2.2. CFBG Edge Filter Interrogation Technique

The CFBG edge filter interrogation technique is similar to the twins FBGs interrogation technique, but it replaces the filter FBG with a chirped fiber Bragg grating (CFBG), as shown in figure 5. The reflected spectra of a CFBG are illustrated in figure 6(a). In the inset of figure 6(a), it can be observed that the rising and falling edges of the reflected spectra of a CFBG are somewhat linear. These linearly rising or falling edges of a CFBG are utilized as a filter and referred to as edge filters.

Figure 6(b) and 6(c) depict the schematic of a CFBG as an edge filter and the respective output when the rising edge is employed as a filter. The maximum temperature range of the sensor interrogated by the CFBG-FBG interrogation technique depends on the wavelength span ( $\Delta\lambda_B$ ) of the linear rising or falling edge and the temperature sensitivity of the sensor.

The sensing range of the FBG temperature sensor can be enhanced by either increasing the rising or falling edge window or by lowering the temperature sensitivity of the sensor. With a rising edge window of 2.1 nm (as shown in the inset of figure 6(a)), the temperature sensing range of the interrogation technique can be calculated using equation (18) as 148.09 °C. However, it has been reported that the temperature sensing range of the CFBG-FBG interrogation technique can reach up to 181.50 °C. To compensate for intensity fluctuations of the source, the rational output method, as given by equation (19), is used.

In a recent study by J. Li et al.[39], they replaced the twin FBGs with a CFBG in their developed interrogation technique and utilized it for strain and temperature sensing. For temperature sensing, they tested their device interrogator in a temperature range from 35 °C to 80 °C with a sensitivity of 0.447 mV/°C. In another study conducted by our research group, we employed the rising edge of the CFBG as an edge filter and achieved temperature sensing up to 181.50 °C. The temperature sensitivity of our technique was 5 mV/°C, and we achieved a resolution of 0.120 °C[38].

**3.2.3. LPG Edge Filter Interrogation Technique**

The transmitted spectra of long period gratings (LPGs) exhibit spectral losses at certain wavelengths. These regions of the LPG spectra with spectral losses can be utilized as edge filters, similar to the rising and falling edges of a CFBG, to convert wavelength shifts into variations in reflected power or intensity of an FBG. Figure 7(a) provides a schematic representation of the interrogation technique employing an LPG as an edge filter. In this technique, the reflected power of an FBG depends on the transmitted power of the LPG at its rising or falling edge. When the rising edge of the LPG is used as a filter (as shown in figure 7(c)), the reflected power of the FBG is initially low at room temperature. As the temperature increases, the Bragg spectra of the FBG shifts towards higher wavelengths, resulting in an increase in the reflected power. Therefore, the shift in the Bragg wavelength of the FBG is demodulated as power or intensity variation, which is then converted to voltage variation using a photodiode and data acquisition card (DAC). On the other hand, if the falling edge of the LPG spectra is used as an edge filter (as shown in figure 7(c)), the reflected power of the sensing FBG decreases with an increase in temperature.

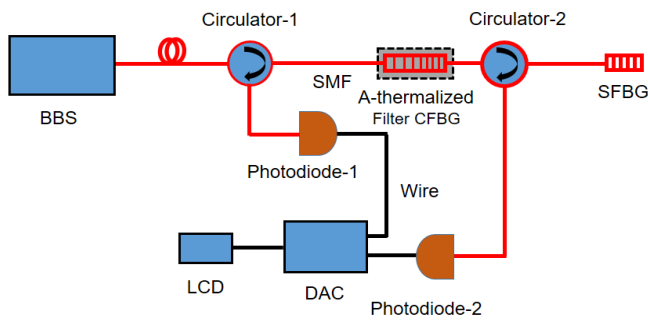


Figure 5. Schematic representation of CFBG-FBG Interrogation Technique for FBG Sensors [38].

In a study by V.R. Pachava et al.[37], they utilized an LPG as an edge filter in their developed interrogation technique for an FBG pressure sensor. They achieved a pressure sensitivity of 90.6 pm/psi and a resolution of 0.025 psi. M.V Reddy et al.[41] developed an FBG temperature sensor package based on an LPG as an edge filter. They achieved high-temperature sensing up to 1000 °C with a resolution of 2 °C. V.R Mamidi et al.[19] developed an FBG high-temperature sensor package using a copper capillary as an encapsulation and an LPG as an edge filter. They achieved high-temperature sensing up to 550 °C with a sensitivity of approximately 1 mV/°C and a resolution of 0.5 °C. Y. Zhan et al.[42] developed a cost-effective FBG high-temperature sensor and employed the LPG edge filter interrogation technique. They achieved high-temperature sensing up to 800 °C with a resolution of 1 °C.

Compared to CFBGs, the span of edges in LPGs is larger, typically ranging from 10-15 nm. This characteristic has been leveraged in the LPG-FBG interrogation technique reported by V.R. Mamidi et al. for temperature sensing up to 550 °C[19]. In this technique, the larger span of edges in the LPG is utilized. To compensate for intensity fluctuations of the source, the rational output method given in equation (19) is also employed in this interrogation technique.

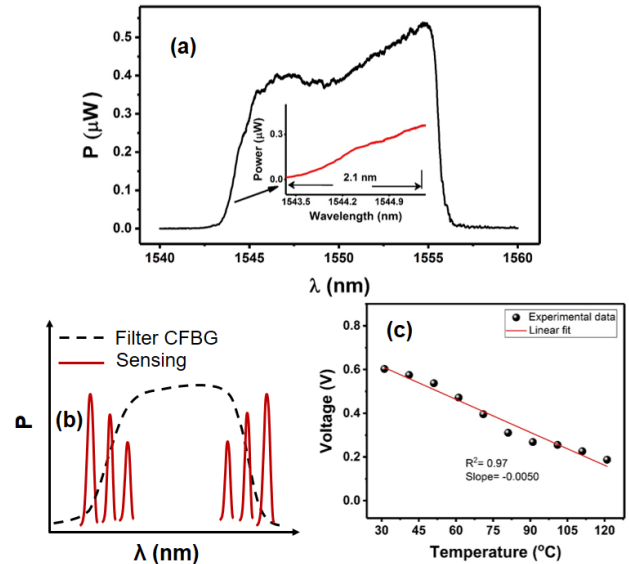


Figure 6. (a) Original reflection spectra of a 1550 nm centered CFBG. Inset represents rising edge of reflection spectra of the CFBG[40] (b) Dotted curve represents reflection spectra of CFBG and reflection spectra of SFBG after filtering from rising and falling edges of CFBG and (c) Output of CFBG-FBG interrogation technique after being filter from rising edge of the CFBG[38].

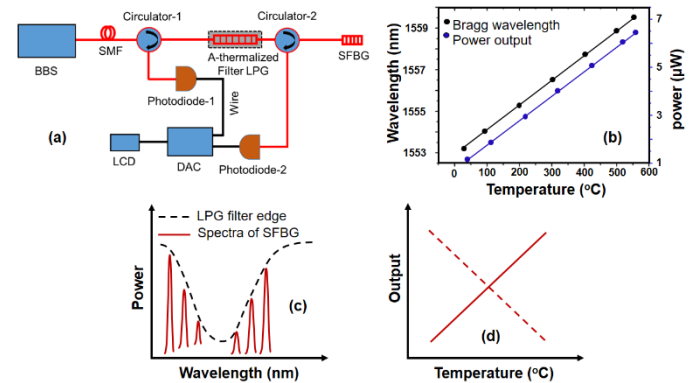


Figure 7. (a) Schematic representation of LPG-CFBG interrogation technique for FBG sensors. (b) Variation of output power with shift in Bragg wavelength of the sensing FBG with increase in temperature. (c) Dotted curve represents reflection spectra of LPG and solid curves represent reflection spectra of SFBG after filtering from rising and falling edges of the LPG (d) Output of LPG-FBG interrogation technique in term of voltage. Solid line represent output when rising edge is used while dotted line represent when falling edge is used [19].

**3.3. Time Division Multiplexing (TDM)**

In time division multiplexing (TDM), the time it takes for a signal from the gratings to return to the detector unit, also known as the time of flight, is measured and converted into the spatial distribution of FBGs. Figure 8(a) illustrates the TDM setup for FBG sensors.

TDM typically utilizes a pulse broadband light source and gratings with the same Bragg wavelength[43]. However, instead of a broadband

source, a laser source can also be used. The light signal from the pulse broadband light source or laser source is transmitted to an array of FBGs, which reflect a combination of signals from different spatially distributed FBGs in the network. Due to the physical separations of the FBGs, the reflected wavelengths reach the detector unit at different times, as depicted in Figure 8(b). This modulated signal in the time domain is then transformed into the wavelength domain and further analyzed to extract sensing information from each individual FBG. Each FBG sensor in the array is identified by the time it takes for its reflected signal to reach the detector unit. In the detector unit, a high-speed spectrometer or a fast photodiode, accompanied by a high-speed oscilloscope, is typically used. These instruments are capable of individually identifying the signal from each FBG in the array [44].

B. Dong et al. [45] proposed a simple TDM technique with a high signal-to-noise ratio. Their developed TDM technique utilizes a tunable pulse fiber laser and a photodiode as key components. Y. Dai et al. [46] proposed a TDM technique for strain and temperature measurement. In their technique, they employed a semiconductor optical amplifier as a gain medium and a switch. Their proposed technique can multiplex up to 100 FBGs, limited by the available bandwidth. Y. Wang et al. [47] utilized an automated fabrication system to produce 1000 ultra-weak gratings and demonstrated TDM for distributed temperature sensing. The resolution of their distributed system is less than 20 pm, corresponding to 2 °C. H. Guo et al. [48] developed a multiplexed network of 3010 nearly identical gratings using TDM. They studied crosstalk between these gratings by employing a commercial interrogator. They attempted to observe and address the crosstalk problem in TDM by highlighting its similarity and symmetry with ghost gratings.

TDM has a dominant advantage over other multiplexing techniques for FBG sensors that it can multiplex thousands of FBG sensors [47, 48]. However, TDM has some limitations which make it less attractive in practical applications which are:

- **Similar wavelength:** In TDM, FBGs with similar Bragg wavelength and partial reflectivity are required.
- **Spatial Separation:** In TDM, the spatial separation between FBGs is a critical consideration. Since time is directly related to distance, it is important to ensure that the signals from each FBG have enough time to be distinguished by the detector unit. In order to achieve this, FBGs in TDM are typically arranged with a spatial separation of meters. This allows for proper differentiation and identification of the individual FBG signals [48].
- **Crosstalk:** Crosstalk refers to the distortion of spectral signals caused by false signals in TDM. These false signals are generated due to multiple reflections between upstream FBGs in an array. The false signal arrives at the detector unit simultaneously with the signals from the downstream FBGs. Crosstalk in TDM leads to the distortion of the real signal and decreases the signal-to-noise ratio. This is a significant concern, especially when dealing with FBGs that have partial or weak reflection [48, 49].
- **Spectral shadowing:** Spectral shadowing refers to the spectral losses experienced by downstream FBGs in an array, which leads to a decrease in the input signal received by the FBGs in the upstream. As a result of spectral shadowing, the signal-to-noise ratio for FBGs in the downstream is reduced. This can have a negative impact on the accuracy and reliability of the measurements obtained from the downstream FBGs in TDM applications.

### 3.4. OSA-Interrogation and Wavelength Division Multiplexing (WDM) Technique

The OSA-based interrogation technique is a commonly used method for FBG sensors, particularly in laboratory research settings. This technique involves directly measuring the Bragg wavelength of the FBG. It utilizes a broadband source of light, such as a amplified spontaneous emission (ASE) source or super-luminescent light emitting diode (SLED) and an OSA for analysis.

In this technique, light from the broadband source is launched into a Single Mode Fiber (SMF) towards a sensing FBG (SFBG). The SFBG reflects a specific wavelength known as the Bragg wavelength or central wavelength. When temperature of the surrounding

environment of the SFBG changes, Bragg wavelength also shifts accordingly. The OSA is used to display the reflected spectra of the FBG, allowing for the detection and analysis of the Bragg wavelength variation. The OSA can be interfaced with a personal computer (PC) for programming and temperature display of the surrounding environment of the FBG. This interrogation technique provides a straightforward and convenient method for monitoring and analyzing the responses of FBG sensors in various research applications.

S. Daud et al. [50] conducted an experimental study to develop a temperature sensor for measuring outdoor temperatures. They used a tunable laser as a source of broadband light and an Optical Spectrum Analyzer (OSA) for their analysis. By varying the temperature from 25°C to 41°C, they observed changes in the reflection and transmission spectra of an FBG. The average temperature sensitivity of their sensor was found to be 10.6 pm/°C for the reflection spectra and 9.1 pm/°C for the transmission spectra. These findings provide valuable insights for the practical application of their temperature sensor in outdoor settings.

S. Spolit et al. [51] conducted a study to investigate three temperature sensor networks consisting of FBGs with different Bragg wavelengths. They examined the temperature range from -20°C to 40°C. In their experiment, they utilized an amplified stimulated emission Broadband Source (BBS) as a light source and employed an Optical Spectrum Analyzer (OSA) as an interrogator. The main focus of their investigation was to determine the minimum spacing intervals required for the FBG sensors to accurately function within the aforementioned temperature range. They conducted experiments under various network scenarios to evaluate this parameter.

S. K. Idris et al. [52] undertook an experimental study using an Optical Spectrum Analyzer (OSA) as an interrogator and a pigtail laser as a light source to investigate the behavior of FBGs in different liquid temperatures and densities. Their findings led them to conclude that FBGs are well-suited for liquid temperature sensing and monitoring applications. By analyzing the reflection and transmission spectra of the FBGs, the researchers were able to observe and measure changes in wavelength that corresponded to variations in temperature and density of the liquid medium. These results indicate that FBGs possess the necessary sensitivity and accuracy to effectively measure liquid temperatures, making them a promising choice for various industries and scientific fields.

J. Roths et al. [53] utilized an Optical Spectrum Analyzer (OSA) to calibrate a Fiber Bragg Grating (FBG) temperature sensor in a cryogenic temperature environment. The temperature range explored in the study spanned from 300 K (room temperature) down to an extremely low temperature of 2.2 K. By employing the OSA, the researchers were able to accurately measure and analyze the wavelength shift of the FBG sensor at various temperature points within the cryogenic range. This enabled them to establish a precise calibration curve, correlating the wavelength shift with the corresponding temperature. The utilization of the OSA for calibration purposes ensured a high level of accuracy and reliability in determining the temperature readings of the FBG sensor in the cryogenic environment. This study underscores the suitability of FBG temperature sensors for use in extreme temperature conditions and demonstrates the effectiveness of the OSA as an invaluable tool for calibration in such environments.

Figure 10(a) depicts the variations in the Bragg spectra of an FBG as temperature increases, as recorded by an Optical Spectrum Analyzer (OSA). The graph clearly shows that higher temperatures cause a linear red shift in the Bragg spectra of the FBG. This shift can be attributed to the temperature-dependent changes in the refractive index of the FBG. Figure 10(b) illustrates the linear relationship between the Bragg wavelength and temperature. By calibrating the shift in the Bragg wavelength of the FBG with the corresponding change in temperature, it can be effectively used as a temperature sensor. This calibration process enables accurate temperature sensing, as the linear relationship between the Bragg wavelength and temperature allows for precise determination of temperature values based on the observed wavelength shifts. Utilizing the FBG as a temperature sensor, calibrated with the shift in the Bragg wavelength, offers a reliable and efficient method for temperature measurement

and monitoring applications. Mathematically, variation of Bragg wavelength with temperature is:

$$\lambda_B = mT + c \tag{11}$$

where, 'm' is slope of the line which gives temperature sensitivity of the sensor in units of pm/°C and 'c' is y-intercepts whose value depends on Bragg wavelength of the FBG. OSA interrogation technique is more reliable, independent of intensity fluctuations of light source and can be used for high temperature sensing. Conventional OSAs have comparatively low resolution, bit slow response speed, costly and large in size. However, modern OSAs are immune from these limitations but still have comparatively high cost than other interrogation techniques. OSAs with wavelength span up to hundreds of nanometers are commercially available therefore temperature sensing range for OSA interrogation calculated by equation (18) is in thousands of celsius.

In Wavelength Division Multiplexing (WDM) systems, multiple fiber Bragg gratings (FBGs) with different Bragg wavelengths are connected to a single fiber, using a single light source and a single monitoring unit. Typically, a Broadband Source (BBS) with a wide bandwidth and a spectrometer are employed in WDM setups. The spectrometer used in WDM systems is equipped with array waveguide gratings (AWG), which allow for the simultaneous interrogation of multiple gratings with fast response[56]. Figure 11(a) shows a schematic of a WDM setup using a BBS and a spectrometer. The BBS launches a broad spectrum of light into the connected fiber, which then passes through an array of FBGs with different Bragg wavelengths.

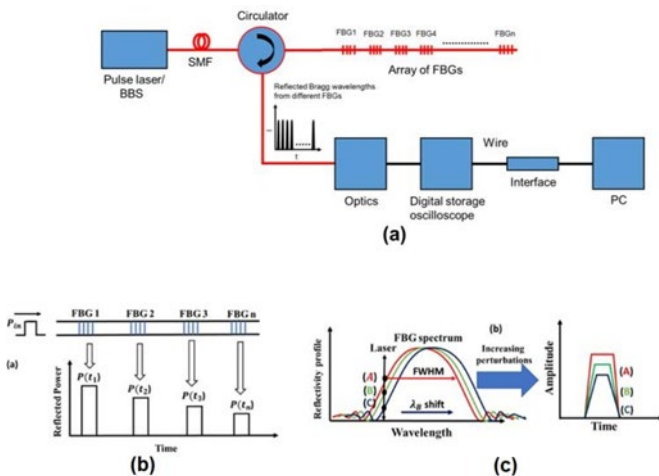


Figure 8. (a) Schematic diagram of TDM interrogation technique for FBG temperature sensors. (b) Representation of working principle of TDM. (c) Conversion of wavelength shift into amplitude variation [54].

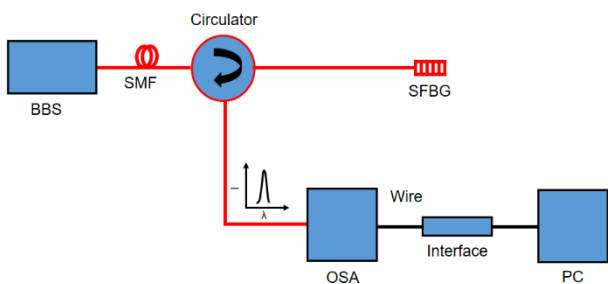


Figure 9. Schematic of OSA Interrogation technique for fiber Bragg grating Temperature sensors

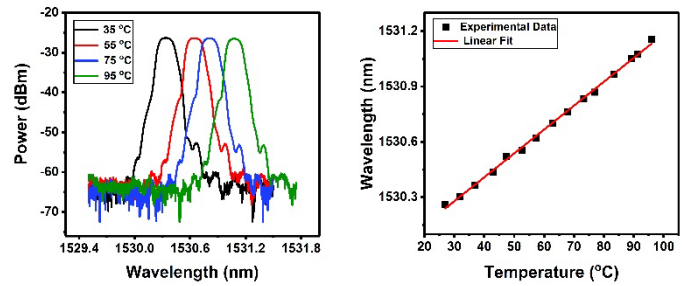


Figure 10. (a) Shift in Bragg spectra of an FBG with increase in its temperature from 40 °C to 100 °C recorded by an OSA (EXFO Electro Optical Engineering Inc., Canada). (b) Linear variation in Bragg wavelength with increase in temperature[55].

Each FBG reflects a specific wavelength, which is directed towards the spectrometer via a three-arm optical circulator. The spectrometer displays the reflected wavelengths from all FBGs simultaneously. Figure 11(b) illustrates the Bragg spectra of seven FBGs as displayed on the spectrometer. When the temperature of an FBG varies, it causes a shift in its respective Bragg wavelength on the spectrometer. To utilize the FBGs as temperature sensors, the shift in the Bragg wavelength of each FBG with temperature is individually calibrated. This calibration process allows for accurate temperature measurements using the FBGs. In most cases, the spectrometer is interfaced with a personal computer (PC) for programming, calibration, and temperature display purposes. This allows for convenient control and monitoring of the WDM system.

Z. Luo et al.[57] reported a theoretical and experimental study on Wavelength Division Multiplexing (WDM) using 2000 ultra-weak Fiber Bragg Gratings (FBGs). In their setup, they utilized two Semiconductor Optical Amplifiers (SOAs) and a high-speed Charge Coupled Module (CCM) as a demodulator. Their proposed sensor network demonstrated high multiplexing capability, allowing for the simultaneous use of 2000 FBGs. The network achieved a spatial resolution of 2 meters and exhibited low insertion loss.

Y.E. Marin et al.[58] developed a WDM interrogator based on a Mach-Zehnder interferometer and validated its performance by comparing it with a commercially available WDM interrogator based on a spectrometer. In their experimental study focused on strain sensing, they achieved a resolution of 4.56 nε/√Hz and a minimum strain detection limit of approximately 0.49 με at a 1-kHz bandwidth using their developed interrogation technique.

M. Teshima et al.[56], proposed a WDM circuit with a stability of 30 MHz and a resolution of 10 MHz. For their experiment, they utilized four tunable lasers as the light source and array waveguide gratings (AWG) for the simultaneous monitoring of multiple wavelengths.

WDM technology allows for the simultaneous measurement of temperature in different objects using a single light source and monitoring unit. Additionally, WDM enables the monitoring of various physical quantities such as pressure, strain, and more, making FBG sensors unique compared to traditional electrical sensors. This multiplexing capability also helps reduce the instrument cost per sensor, as thousands of FBG sensors can be multiplexed [58]. The number of sensors that can be multiplexed depends on three factors: the power of the broadband source (BBS), the bandwidth of the BBS's light spectra, and the wavelength detection window of the spectrometer. To ensure accurate temperature sensing, it is important to have a sufficient difference in Bragg wavelength between consecutive FBGs so that their spectra do not overlap when temperature changes occur. FBGs can be multiplexed in the form of a single array, multiple arrays, or in a tree topology, depending on the specific application. Commercially available interrogators that employ WDM typically have a wavelength span of 80 nm, allowing for a temperature detection range of approximately 5000 °C, as calculated by equation (18).



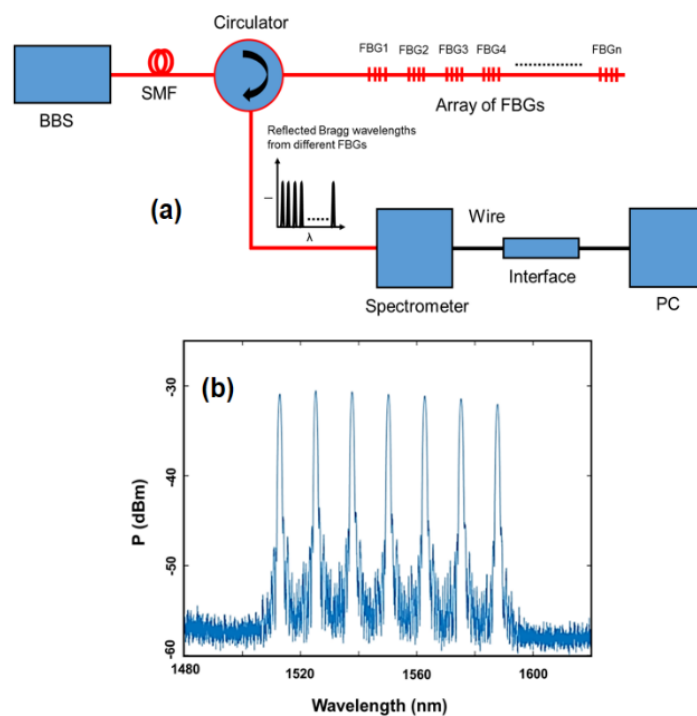


Figure 11. Schematic of WDM of n-FBGs with different Bragg wavelengths employing a BBS and a spectrometer. (b) Bragg spectra of 7 FBGs connected in an array. Each peak represents an individual FBG sensor[59].

Table 1. Comparison of different Interrogation Techniques for FBG Temperature Sensors

Interrogation Technique	Resolution	Range	Cost per sensor	Multiplexing capacity	Commercial Interrog-ators	Reference
Interferometry	High	0-60 °C	Low	–	–	[35]
Optical filter	Twin FBGs (0.3 pm)	0-20 °C	Low	–	–	[36, 38]
	CFBG-FBG (0.3 pm)	0-181.50 °C	Low	–	–	[38]
	LPG-FBG (1.4 pm)	20-550 °C	Low	–	–	[19]
TDM	–	–	Low	High	Applied	–
OSA	4.93 °C (70 pm)	0-7000 °C (for 100nm span)	High	Medium	Research purpose	[60]
WDM	0.09 °C (1.26 pm)	0-5000 °C	Low	medium	Applied	[61]

4. Conclusions

This comprehensive review delves into the realm of FBG temperature sensors and their interrogation techniques. Through an in-depth exploration, we have unveiled a range of novel strategies applicable to diverse industrial and research environments. The distinct advantages and limitations of interrogation techniques such as optical interferometry, optical edge filtering, time division multiplexing, optical spectrum analysis, and wavelength division multiplexing have been dissected. By elucidating the strengths and weaknesses of different interrogation techniques, we aim to guide researchers, engineers toward the development of optimized FBG-based temperature sensing solutions. Through our findings, we aspire to stimulate further innovation and inspire collaborative efforts that drive the advancement of temperature sensing technologies.

Declaration of Conflict of Interests

The authors declare that there is no conflict of interest. They have no known competing financial interests or personal relationships that could have appeared to influence the work reported in this paper.

References

- [1.] D. S. Glazier, Is metabolic rate a universal ‘pacemaker’ for biological processes?. *Biological Reviews* 90 (2015) 377-407.
- [2.] T. D. McGee, Principles and methods of temperature measurement. John Wiley & Sons, (1988).
- [3.] P. R. N. Childs, J. R. Greenwood, and C. A. Long, Review of temperature measurement. *Review of scientific instruments* 71 (2000) 2959-2978.
- [4.] P. R. N. Childs, Practical temperature measurement. Elsevier (2001).
- [5.] M. M. Werneck, R. Allil, B. A. Ribeiro, and F. V. B. de Nazaré, A guide to fiber Bragg grating sensors. *Current trends in short-and long-period fiber gratings* (2013)1-24.

- [6.] Z. Zhou, T. W. Graver, L. Hsu, and J.-p. Ou, "Techniques of Advanced FBG sensors: fabrication, demodulation, encapsulation and their application in the structural health monitoring of bridges," *Pacific Science Review* 5 (2003)116-121.
- [7.] B. Xu et al., Femtosecond laser point-by-point inscription of an ultra-weak fiber Bragg grating array for distributed high-temperature sensing. *Optics Express* 29 (2021)32615-32626.
- [8.] J. He, B. Xu, X. Xu, C. Liao, and Y. Wang, "Review of femtosecond-laser-inscribed fiber bragg gratings: Fabrication technologies and sensing applications," *Photonic Sensors* 11 (2021)203-226.
- [9.] R. Ullah, R. Y. M. Khan, and M. Faisal, "Efficient diaphragm-based Fiber Bragg grating vacuum sensor," *Vacuum*, (2023) 111566.
- [10.] R. Rajini-Kumar, M. Suesser, K. G. Narayankhedkar, G. Krieg, and M. D. Atrey, Performance evaluation of metal-coated fiber Bragg grating sensors for sensing cryogenic temperature, *Cryogenics* 48 (2008) 142-147.
- [11.] U. Sampath, D. Kim, H. Kim, and M. Song, Polymer-coated FBG sensor for simultaneous temperature and strain monitoring in composite materials under cryogenic conditions. *Applied optics* 57 (2018) 492-497.
- [12.] S. Parne, R. L. N. Sai Prasad, S. G. Dipankar, M. Sai Shankar, and S. Kamineni, Polymer-coated fiber Bragg grating sensor for cryogenic temperature measurements. *Microwave and optical technology letters*, vol. 53 (2011) 1154-1157.
- [13.] D. Sengupta, M. S. Shankar, P. S. Reddy, R. L. N. S. Prasad, K. S. Narayana, and P. Kishore, An improved low temperature sensing using PMMA coated FBG : *Optica Publishing Group* (2011) 831103.
- [14.] R. Rajinikumar, A. Nyilas, M. Süsser, and K. G. Narayankhedkar, Investigation of fiber Bragg grating sensors with different coating materials for high sensitivity. *Proc ICEC* 21 (2006) 467-470.
- [15.] R. A. Freitas, *Optical fiber temperature sensors for cryogenic applications. Universidade do Porto (Portugal)* (2013).
- [16.] C.-Y. Hsu, C.-C. Chiang, T.-S. Hsieh, H.-C. Hsu, L. Tsai, and C.-H. Hou, Study of fiber Bragg gratings with TiN-coated for cryogenic temperature measurement. *Optics & Laser Technology* 136 (2021), pp. 106768.
- [17.] A. C. Soman, A. T. Chalackal, and S. Kanakambaran, Design of Cryogenic Temperature Sensors using Copper-Coated Fiber Bragg Gratings. *IEEE* (2022) 1-5.
- [18.] V. R. Mamidi, S. Kamineni, L. N. S. P. Ravinuthala, V. Thumu, and V. R. Pachava, Characterization of encapsulating materials for fiber bragg grating-based temperature sensors. *Fiber and Integrated Optics* 33 (2014) 325-335.
- [19.] V. R. Mamidi et al., "Fiber Bragg grating-based high temperature sensor and its low cost interrogation system with enhanced resolution," *Optica Applicata*, vol. 44, no. 2, pp. 299--308, 2014.
- [20.] R. Y. M. Khan, R. Ullah, and M. Faisal, Design and development of type-1 FBG based high temperature sensor. *Physica Scripta* 98 (2023) 045515.
- [21.] P. Lu, L. Men, and Q. Chen, Polymer-coated fiber Bragg grating sensors for simultaneous monitoring of soluble analytes and temperature. *IEEE Sensors Journal* 4 (2009) 340-345.
- [22.] L. Huang, R. S. Dyer, R. J. Lago, A. A. Stolov, and J. Li, "Mechanical properties of polyimide coated optical fibers at elevated temperatures," 2016, vol. 9702, pp. 177-184: SPIE.
- [23.] S. L. Semjonov, M. M. Bubnov, E. M. Dianov, and A. G. Shchebunyaev, Reliability of aluminum-coated fibers at high temperature. *SPIE* 2074 (1994)25-33.
- [24.] K. N. Koo et al., Fabrication and modification of temperature FBG sensor: role of optical fiber type and Cu sputtered thickness. *Physica Scripta* 95 (2020)095509.
- [25.] N. F. Mansor and R. K. R. Ibrahim, Temperature sensitivity of FBG coating with zinc oxide and silicon carbide. *IOP Publishing* 1892 (2021) 012033.
- [26.] X. Wang, X. Sun, Y. Hu, L. Zeng, Q. Liu, and J. a. Duan, Highly-sensitive fiber Bragg grating temperature sensors with metallic coatings. *Optik* 262 (2022) 169337.
- [27.] N. Groothoff and J. Canning, Enhanced type IIA gratings for high-temperature operation. *Optics letters* 29 (2004) 2360-2362.
- [28.] J. Kumar, G. Singh, M. K. Saxena, O. Prakash, S. K. Dixit, and S. V. Nakhe, Development and studies on FBG temperature sensor for applications in nuclear fuel cycle facilities. *IEEE Sensors Journal* 21 (2020) 7613-7619.
- [29.] C. Zhu, D. Alla, and J. Huang, High-temperature stable FBGs fabricated by a point-by-point femtosecond laser inscription for multi-parameter sensing. *OSA Continuum* 4 (2021) 355-363.
- [30.] N. Chanet et al., Design and integration of femtosecond fiber Bragg gratings temperature probes inside actively cooled ITER-like plasma-facing components. *Fusion Engineering and Design* 166 (2021) 112.
- [31.] M. Wang et al., Femtosecond laser fabrication of nanograting-based distributed fiber sensors for extreme environmental applications. *International Journal of Extreme Manufacturing* 3 (2021) 025401.,
- [32.] A. Martinez, I. Y. Khrushchev, and I. Bennion, Thermal properties of fibre Bragg gratings inscribed point-by-point by infrared femtosecond laser. *Electronics letters* 41 (2005) 176-178.
- [33.] T. Habisreuther, T. Elsmann, Z. Pan, A. Graf, R. Willsch, and M. A. Schmidt, Sapphire fiber Bragg gratings for high temperature and dynamic temperature diagnostics. *Applied Thermal Engineering* 91 (2015) 860-865.
- [34.] B. Das and V. Chandra, Fiber-MZI-based FBG sensor interrogation: comparative study with a CCD spectrometer. *Applied Optics* 55 (2016) 29 8287-8292.
- [35.] M. Perry, P. Orr, P. Niewczas, and M. Johnston, High-speed interferometric FBG interrogator with dynamic and absolute wavelength measurement capability. *Journal of lightwave technology* 31 (2013) 2897-2903.
- [36.] J. Cui, Y. Hu, K. Feng, J. Li, and J. Tan, FBG Interrogation Method with High Resolution and Response Speed Based on a Reflective-Matched FBG Scheme. *Sensors* 15 (2015) 16516-16535.
- [37.] V. R. Pachava, S. Kamineni, S. S. Madhuvarasu, K. Putha, and V. R. Mamidi, FBG based high sensitive pressure sensor and its low-cost interrogation system with enhanced resolution. *Photonic Sensors* 5 (2015) 321-329.
- [38.] R. Y. M. Khan, R. Ullah, and M. Faisal, Design and Development of Cost-effective FBG Temperature Sensor Package. *Measurement Science and Technology* (2023).

- [39.] J. Li, C. Lu, F. Zeng, Y. Zhang, S. Li, and W. Sun, Range extension method for reflective-matched FBG interrogation based on CFBG sensor. *Optical Fiber Technology* 75 (2023) 103210.
- [40.] R. Ullah, R. Y. Mehmood Khan, and M. Faisal, Design and development of an economical temperature compensated bidirectional fiber Bragg grating flow sensor. *Engineering Research Express* (2023).
- [41.] V. Reddy, K. Srimannarayana, R. L. N. S. Prasad, and T. V. Apparao, FBG-based novel sensor for high-temperature measurement and its low-cost interrogation. *SPIE 2015* 9506 (2015) 76-81.
- [42.] Y. Zhan, S. Xue, Q. Yang, S. Xiang, H. He, and R. Zhu, A novel fiber Bragg grating high-temperature sensor. *Optik* 119 (2008) 535-539.
- [43.] L. C. S. Nunes, B. S. Olivieri, C. C. Kato, L. C. G. Valente, and A. M. B. Braga, FBG sensor multiplexing system based on the TDM and fixed filters approach. *Sensors and Actuators A: Physical* 138 (2007) 341-349.
- [44.] J. C. C. Chan, Interrogation of fiber Bragg grating sensors with a tunable laser source. *Hong Kong Polytechnic University (Hong Kong)* (2000).
- [45.] B. Dong, S. He, S. Hu, D. Tian, J. Lv, and Q. Zhao, Time-division multiplexing fiber grating sensor with a tunable pulsed laser. *IEEE photonics technology letters* 18 (2006) 2620-2622.
- [46.] Y. Dai, G. Deng, J. Leng, and A. Asundi, Time division multiplexing of FBG sensor system. *SPIE* 7375 (2009) 1055-1059.
- [47.] Y. Wang, J. Gong, B. Dong, D. Y. Wang, T. J. Shillig, and A. Wang, A large serial time-division multiplexed fiber Bragg grating sensor network. *Journal of Lightwave Technology* 30 (2012) 2751-2756.
- [48.] H. Guo et al., Crosstalk and ghost gratings in a large-scale weak fiber Bragg grating array. *Journal of Lightwave Technology* 35 (2016) 2032-2036.
- [49.] S. Wu, H. Wen, and X. Chen, Method for reducing the influence of crosstalk on quasi-distributed sensing network with time-division multiplexing fibre Bragg gratings. *IOP Publishing* 1754 (2021) 012212.
- [50.] S. Daud, M. A. Jalil, S. Najmee, S. Saktioto, J. Ali, and P. P. Yupapin, Development of FBG sensing system for outdoor temperature environment. *Procedia Engineering* 8 (2011) 386-392.
- [51.] S. Spolitis, I. Lyashuk, and V. Bobrovs, Design and performance evaluation of FBG-based temperature sensors network. *IEEE* (2017) 2673-2678.
- [52.] S. K. Idris, H. Haroon, H. A. Razak, and A. S. M. Zain, Investigation on fiber optic sensor using FBG for various temperature and liquid density. *IOP Publishing* 1502 (2020) 012009.
- [53.] J. Roths, G. Andrejevic, R. Kuttler, and M. Süßer, Calibration of fiber Bragg cryogenic temperature sensors. *Optica Publishing Group* (2006) TuE81.
- [54.] M. M. Elgaud et al., Digital Filtering Techniques for Performance Improvement of Golay Coded TDM-FBG Sensor. *Sensors* 21 (2021) 4299.
- [55.] D.-M. Han et al., Observation of the standing wave effect in large-area, very-high-frequency capacitively coupled plasmas by using a fiber Bragg grating sensor. *Journal of Applied Physics* 123 (2018) 223304.
- [56.] M. Teshima, M. Koga, and K. Sato, Multiwavelength simultaneous monitoring circuit employing wavelength crossover properties of arrayed-waveguide grating. *Electronics Letters* 31 (1995) 1595-1597.
- [57.] Z. Luo, H. Wen, H. Guo, and M. Yang, A time-and wavelength-division multiplexing sensor network with ultra-weak fiber Bragg gratings. *Optics Express* 21 (2013) 22799-22807.
- [58.] Y. E. Marin et al., Integrated dynamic wavelength division multiplexed FBG sensor interrogator on a silicon photonic chip. *Journal of Lightwave Technology* 37 (2019) 4770-4775.
- [59.] M. Zaltieri, G. Allegretti, C. Massaroni, E. Schena, and F. M. Cauti, Fiber bragg grating sensors for millimetric-scale temperature monitoring of cardiac tissue undergoing radiofrequency ablation: A feasibility assessment. *Sensors* 20 (2020) 6490.
- [60.] S. D. Dyer, P. A. Williams, R. J. Espejo, J. D. Kofler, and S. M. Etzel, Fundamental limits in fiber Bragg grating peak wavelength measurements. *SPIE* 5855 (2005) 88-93.
- [61.] P. C. Silveira et al., Experimental evaluation of low-cost interrogation techniques for FBG sensors. *IEEE* (2018) 1-6.

### How to Cite This Article

R. Y. M. Khan, R. Ullah, and M. Faisal, Fiber Bragg Grating Temperature Sensor and its Interrogation Techniques, *Brilliant Engineering*, 3 (2023),4840.  
<https://doi.org/10.36937/ben.2023.4840>.